

Anomalous phonon shifts in the paramagnetic phase of multiferroic RMn_2O_5 ($R=Bi, Eu, Dy$): Possible manifestations of unconventional magnetic correlations

A. F. García-Flores,¹ E. Granado,^{1,*} H. Martinho,² R. R. Urbano,¹ C. Rettori,¹ E. I. Golovenchits,³ V. A. Sanina,³ S. B. Oseroff,⁴ S. Park,⁵ and S.-W. Cheong⁵

¹Instituto de Física “Gleb Wataghin,” UNICAMP, C.P. 6165, 13083-970, Campinas-SP, Brazil

²Instituto de Pesquisa e Desenvolvimento, UNIVAP, 12244-050, São José dos Campos-SP, Brazil

³Ioffe Physical-Technical Institute of RAS, 194021, St. Petersburg, Russia

⁴San Diego State University, San Diego, California 92182, USA

⁵Department of Physics and Astronomy, Rutgers University, Piscataway, New Jersey 08854, USA

(Received 17 October 2005; revised manuscript received 23 January 2006; published 10 March 2006)

A Raman spectroscopic study of the high-frequency optical phonons in single crystals of the multiferroic system RMn_2O_5 ($R=Bi, Eu, Dy$) was performed. All studied materials show anomalous phonon shifts, below a new characteristic temperature for these materials, $T^* \sim 60\text{--}65$ K. The sign and magnitude of such shifts appear to be correlated with the ionic radius of R , involving from softenings for $R=Bi$ to hardenings for $R=Dy$ and showing an intermediary behavior for $R=Eu$. Additional phonon anomalies were identified below $\sim T_N \sim 40\text{--}43$ K, reflecting the onset of long-range ferroelectric and/or magnetic order of the Mn sublattice. Complementary dc-magnetic susceptibility [$\chi(T)$] measurements for $BiMn_2O_5$ up to 800 K yield a Curie-Weiss temperature $\theta_{CW} = -253(3)$ K, revealing a fairly large frustration ratio ($|\theta_{CW}|/T_N = 6.3$). Deviations of $\chi(T)$ from a Curie-Weiss paramagnetic behavior due to magnetic correlations were observed below temperatures of the order of $|\theta_{CW}|$, with the inverse susceptibility showing inflection points at ~ 160 K and $\sim T^*$. Supported by $\chi(T)$ data, the anomalous Raman phonon shifts below T^* are interpreted in terms of the spin-phonon coupling, in a scenario of strong magnetic correlations. Overall, these results support significant magnetic frustration, introduce a new characteristic temperature (T^*), and suggest a surprisingly rich behavior for the magnetic correlations in the paramagnetic phase of this system.

DOI: [10.1103/PhysRevB.73.104411](https://doi.org/10.1103/PhysRevB.73.104411)

PACS number(s): 75.30.Et, 75.50.Ee, 78.30.-j, 63.20.Ls

I. INTRODUCTION

Multiferroics, also termed magnetoelectrics, are materials where (anti)ferromagnetism and (anti)ferroelectricity coexist. Such a rare¹ effect attracts steady attention due to the interesting physics involved as well as relevant potential applications in devices with new functionalities. In multiferroics, a coupling between magnetic and electric properties may in principle occur, leading to concrete possibilities of realizing the long-sought control of the electric polarization by a magnetic field or vice-versa.²⁻⁴ Among other interesting systems, promising candidates for this purpose may be found within the RMn_2O_5 family (R =rare earth, Y, or Bi), which are isostructural insulators.⁵⁻⁷ Members of this family undergo a ferroelectric transition at (or slightly below) the antiferromagnetic (AFM) transition temperature for the Mn spin sublattice, $T_N = 39\text{--}45$ K.⁷⁻¹³ This system is also characterized by the existence of other magnetic transitions at lower temperatures between distinct commensurate and incommensurate Mn spin structures.¹²⁻¹⁵ In addition, the R^{3+} spin system may order below 10 K.^{8,12,14,16,17} Each magnetic transition is in general followed by a corresponding ferroelectric transition, clearly signaling a coupling between magnetic and electric properties.^{8,16} In fact, for $DyMn_2O_5$ and $TbMn_2O_5$, giant magnetoelectric effects have been observed.^{5,8,16,17}

A detailed understanding of the multiferroic properties of the RMn_2O_5 family is challenged by the complex crystal and magnetic structures. Figure 1 shows the crystallographic structure of RMn_2O_5 along the z -axis. $Mn^{4+}O_6$ octahedra

form edge-sharing infinite linear chains along the z direction. $Mn^{3+}O_5$ square pyramids interconnect the $Mn^{4+}O_6$ octahedra. The magnetic structures depend strongly on R and T . All phases show a magnetic propagation vector $(k_x, 0, k_z)$ with $k_x \sim 1/2$.^{7,9,12,13,18} Recently, the magnetic structures of $(Bi, Ho, Tb, Dy)Mn_2O_5$ were studied in detail.^{9,12,13} It was suggested that the lattice geometry causes an inherent magnetic frustration in the system, which is lifted by small shifts of the Mn^{3+} cations.^{12,13} This would lead to a canted antiferroelectric phase that would be strongly coupled to the magnetic structure, providing a hint for the strong magnetoelec-

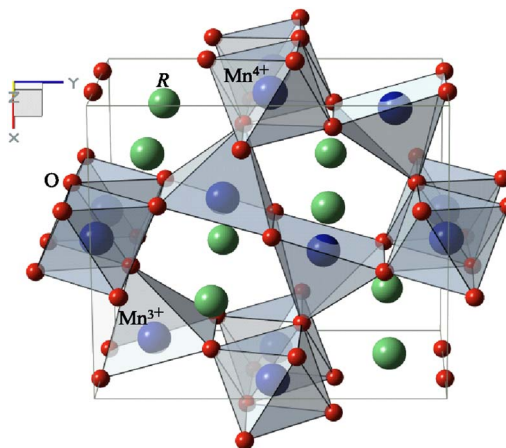


FIG. 1. (Color online) A view of the crystal structure of RMn_2O_5 ($R=Bi, Dy, Eu$) along the z -axis.

tric coupling in this system. If this scenario is correct, strong magnetic correlations are prone to be found above T_N .¹⁹ In fact, in frustrated systems, a detailed investigation of such correlations in the paramagnetic phase may be an essential step towards a satisfactory understanding of the overall physical properties. Nonetheless, few information is presently available on the nature and strength of the magnetic correlations in the paramagnetic phase of multiferroic RMn_2O_5 , to our best knowledge. We note that the complex crystal structure and the presence of distinct magnetic ions (Mn^{3+} , Mn^{4+} , and, in some cases R^{3+}) requires the use of microscopic experimental techniques for a detailed investigation of such correlations.

In this work, we argue that microscopic information of the Mn-Mn spin correlations in the paramagnetic phase of the RMn_2O_5 family ($R=Bi, Eu, \text{ and } Dy$) was achieved by means of a phonon Raman scattering study, complemented by dc-magnetic susceptibility measurements. Anomalous frequency shifts of stretching Mn-O modes were observed below a new characteristic temperature for this system, $T^* \sim 60\text{--}65$ K. Supported by magnetic data in $BiMn_2O_5$, such shifts are ascribed to the spin-phonon coupling, i.e., a modulation of the superexchange energy of specific Mn-O-Mn paths by each vibration. This interpretation implies that a rather abrupt change in the nature or strength of at least some of the Mn-Mn spin correlations takes place at T^* . The sign and magnitude of the anomalous phonon shifts appear to be correlated with the ionic radii of R , involving from softenings for $R=Bi$ to hardenings for $R=Dy$. Such trend appears to indicate distinct magnetic correlations for each R , which is possibly a precursor effect that leads to the distinct long-range-ordered magnetic structures below T_N .

II. EXPERIMENTAL DETAILS

The single crystals used in the present study were prepared by the flux method, as described elsewhere.^{8,20} The Raman scattering spectra were excited with the 514.5 nm laser line from an Ar^+ laser, with a power of ~ 12 mW focused in a spot of ~ 100 μm diameter. All measurements were made in a near-backscattering configuration. The scattered light was analyzed by a triple grating spectrometer equipped with a LN_2 -cooled CCD detector. Measurements were performed in the $80\text{ cm}^{-1} < \omega < 900\text{ cm}^{-1}$ range. The T -dependent measurements were carried out by mounting the samples on a cold finger of a closed-cycle He refrigerator. T -accuracy was better than ~ 2 K. For $R=Bi$ and Eu , $T_N=40$ K was obtained from dc-magnetization measurements, in good agreement with reported values.^{9,14} dc-magnetic susceptibility measurements on $BiMn_2O_5$ were performed under a field of 1 T using a commercial superconducting quantum interference device (SQUID) magnetometer (see footnote²¹).

III. RESULTS AND ANALYSIS

A. Raman scattering

Factor group analysis for the $Pbam$ symmetry of the paraelectric phase of these oxides yields a total of 48 Raman-active phonon modes ($\Gamma_{Raman} = 13A_g + 13B_{1g} + 11B_{2g}$

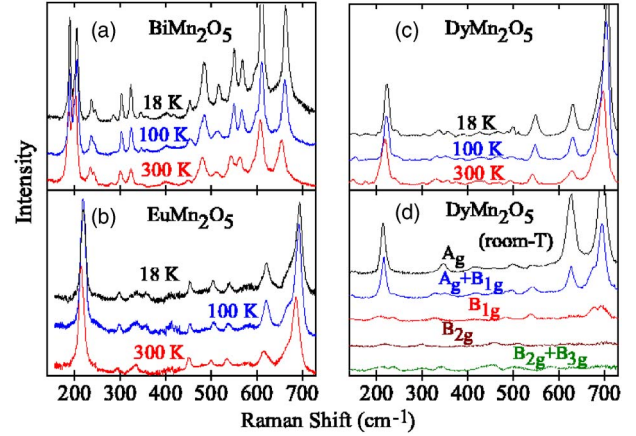


FIG. 2. (Color online) Unpolarized Raman spectra of (a) $BiMn_2O_5$, (b) $EuMn_2O_5$, and (c) $DyMn_2O_5$ at 10, 100, and 300 K. (d) Symmetry-dependence of the Raman spectra of $DyMn_2O_5$ at room- T .

+ $11B_{3g}$).²² Figures 2(a)–2(c) show unpolarized Raman spectra of RMn_2O_5 ($R=Bi, Eu, Dy$) at 18, 100, and 300 K. Only some expected modes were observed for all samples. For $R=Bi$, 19 Raman peaks were seen at 185, 195, 200, 235, 245, 280, 300, 325, 345, 360, 405, 445, 480, 510, 545, 565, 595, 610, and 655 cm^{-1} (room- T). For $R=Eu$, 11 modes were observed at 215, 295, 325, 335, 355, 450, 495, 535, 620, 665, and 685 cm^{-1} (room- T). For $R=Dy$, a polarization analysis was also performed [see Fig. 2(d)], taking advantage of the well defined (001), (110), ($1\bar{1}0$), and (010) natural faces of this particular crystal. 24 modes were then observed, according to the following symmetry assignment: A_g modes at 215, 350, 420, 460, 500, 545, 625, and 695 cm^{-1} ; B_{1g} modes at 145, 205, 235, 330, 420, 485, 540, and 675 cm^{-1} ; B_{2g} modes at 220, 305, 460, and 510 cm^{-1} ; and B_{3g} modes at 320, 440, 495, and 585 cm^{-1} (room- T). This symmetry analysis for $R=Dy$ is in general agreement with previous results of Mikhailova *et al.* for $R=Ho$ and Tb .²³ The overall Raman spectra for $R=Dy$ and $R=Eu$ are very similar, while, for $R=Bi$, the Raman modes are considerably sharper, better defined, and shifted towards lower energies. This trend is more readily realized for the highest energy modes ($>600\text{ cm}^{-1}$). No additional Raman peaks were observed for the low- T ferroelectric phase with respect to the paraelectric phase in any of the studied crystals, suggesting that the ionic displacements associated with the ferroelectric phase are rather small.

Anomalous phonon behavior was detected for all studied crystals. In this work, the analysis is focused on the high-energy modes ($\omega > 500\text{ cm}^{-1}$), which are ascribed to Mn-O stretching vibrations. Figure 3(a) shows a selected portion of the Raman spectra of $BiMn_2O_5$ at several T for a selected frequency interval ($520\text{ cm}^{-1} < \omega < 590\text{ cm}^{-1}$). Figures 3(b)–3(e) show the T -dependence of the frequency of the high-energy modes at 545, 565, 610, and 655 cm^{-1} . Upon cooling, all modes show conventional hardening down to $T^* \sim 65$ K. Below T^* , the studied modes show a clear change in behavior, with an anomalous softening on cooling down to $T_N \sim 40$ K, coincident with the magnetic ordering temperature.⁹ Below T_N , the modes show another change in

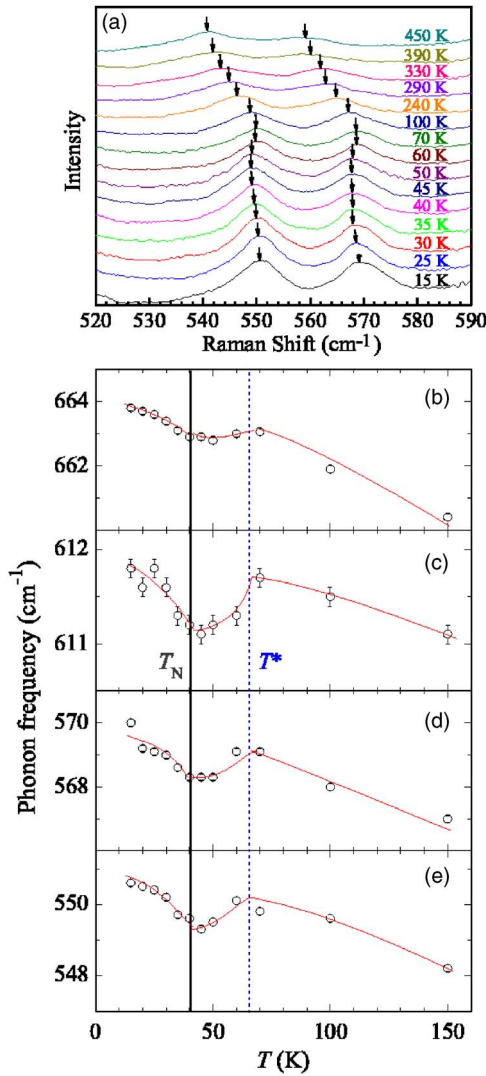


FIG. 3. (Color online) (a) Selected portion of the Raman spectra of BiMn_2O_5 at several temperatures. The mode positions are indicated by arrows as a guide to the eyes. (b)–(e) T -dependencies of the positions of selected high-frequency Raman modes. The solid vertical line represents the anti-ferromagnetic transition temperature [see Refs. 9 and 10 and Fig. 5(a)], while the dashed line indicates T^* , the temperature below which anomalous phonon behavior is observed.

behavior, hardening again upon cooling. We emphasize that the hardening below T_N does not appear to be a conventional phenomenon in this case, since lattice contraction due to anharmonic effects are not expected to be significant in this T -range (Debye temperature ~ 235 K).⁹ The T -dependence of the phonon linewidths (not shown) revealed no clear anomaly at T_N and T^* for all modes, within our experimental resolution.

Figures 4(a) and 4(b) show the T -dependence of the position of the most intense high-frequency Raman modes for $R=\text{Eu}$, at ~ 620 and ~ 690 cm^{-1} . Frequency anomalies, similar to those found for $R=\text{Bi}$ [see Figs. 3(b) and 3(c)], were observed. However, the tendency for phonon softenings between $T^* \sim 65$ K and $\sim T_N = T_c = 40$ K¹⁴ is less pronounced for $R=\text{Eu}$ than for $R=\text{Bi}$, where T_c represents the ferroelec-

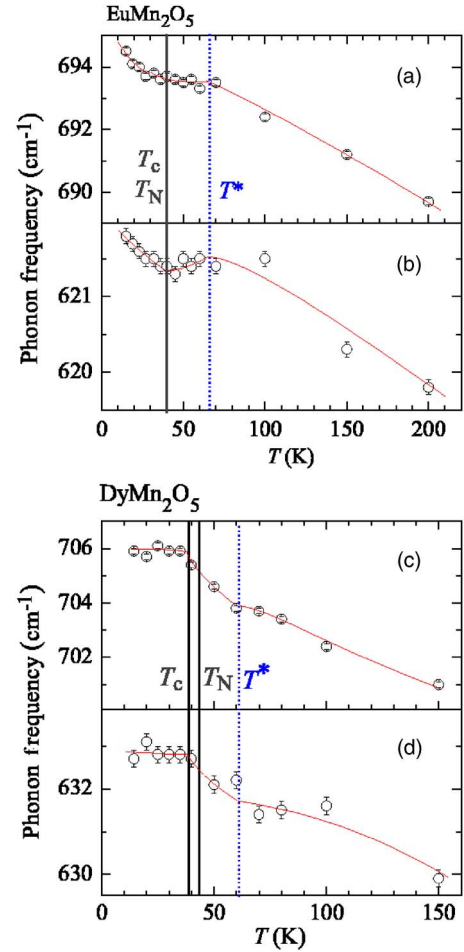


FIG. 4. (Color online) T -dependence of the position of selected high-frequency Raman modes for EuMn_2O_5 (a) and (b) and DyMn_2O_5 (c) and (d). The dashed vertical lines mark T^* , while the solid vertical lines represent the reported antiferromagnetic and ferroelectric ordering temperatures of the Mn sublattice (T_N and T_c , respectively Refs. 8, 14, and 16).

tric transition temperature. On the other hand, the phonon hardenings that take place below $\sim T_N$ and T_c are similar in magnitude for $R=\text{Eu}$ and Bi .

The T -dependencies of the positions of the most pronounced Mn-O stretching modes for $R=\text{Dy}$ are given in Figs. 4(c) and 4(d). The behavior of the mode at ~ 705 cm^{-1} reveals again the existence of two characteristic temperatures, $T^* \sim 60$ K and $\sim T_c = 39$ K, showing a steep hardening upon cooling between T^* and $\sim T_c$, and a nearly constant frequency below $\sim T_c$. The mode at ~ 630 cm^{-1} appears to show a similar behavior, although the larger error bars in this case do not allow for a conclusive statement.

B. Magnetic susceptibility

In order to gain further insight into the nature of the new characteristic temperature T^* evidenced by the phonon shifts in this system, detailed dc-magnetic susceptibility (χ) measurements were performed for BiMn_2O_5 between 2 and 800 K. This particular compound was chosen since Bi^{3+} is

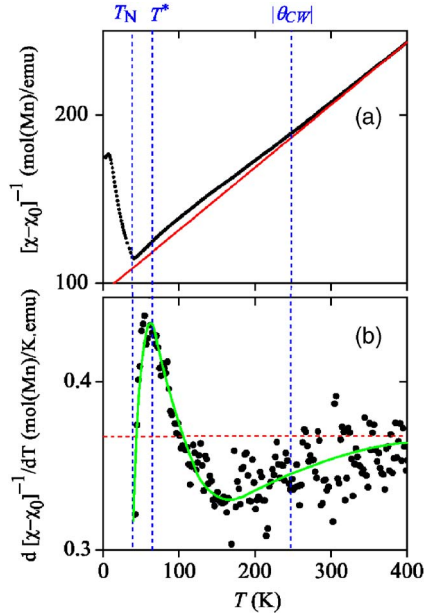


FIG. 5. (Color online) (a) T -dependence of the inverse of the dc magnetic susceptibility $\chi(T)$ of BiMn_2O_5 , after subtraction of a small diamagnetic constant term χ_0 (see text) (symbols). The solid line represents an extrapolation of the Curie-Weiss behavior that matches the data between 400 and 800 K (not shown). (b) T -derivative of $(\chi(T) - \chi_0)^{-1}$ (symbols). The solid line is a guide to the eyes and the horizontal dashed line is the prediction of the Curie-Weiss law. The vertical dashed lines in (a) and (b) mark the Néel temperature (T_N), modulus of the Curie-Weiss temperature ($|\theta_{CW}|$), and the temperature below which anomalous Raman shifts were observed (T^*).

diamagnetic, contributing only with a T -independent portion to the susceptibility. Thus, any interesting feature in $\chi(T)$ must be solely due to the Mn moments for this compound. A fit of the measured $\chi(T)$ curve for $400 \text{ K} < T < 800 \text{ K}$ to the expression $\chi(T) = \chi_0 + C/(T - \theta_{CW})$ (not shown) yields $\chi_0 = -4.2(2) \times 10^{-4} \text{ emu/mol}(\text{BiMn}_2\text{O}_5)$, $C = 2.69(2) \text{ emu.K/mol}(\text{Mn})$, and $\theta_{CW} = -253(3) \text{ K}$. The diamagnetic term obtained from the fit is in agreement with the theoretical prediction $\chi_0^{teo} = -4.06 \times 10^{-4} \text{ emu/mol}(\text{BiMn}_2\text{O}_5)$ (see footnote²⁴). Also, from the observed paramagnetic Curie constant C , an effective moment of $4.64 \mu_B/\text{Mn}$ is obtained, which is between the expected values for Mn^{3+} ($4.90 \mu_B/\text{Mn}$) and Mn^{4+} ($3.87 \mu_B/\text{Mn}$).²⁵ Figure 5(a) shows the inverse susceptibility below 400 K, after subtraction of the experimentally obtained diamagnetic term, $(\chi(T) - \chi_0)^{-1}$. An extrapolation of the Curie-Weiss paramagnetic behavior with the above constants is also displayed. It can be noted that $(\chi(T) - \chi_0)^{-1}$ starts to deviate significantly from the Curie-Weiss behavior at temperatures of the order of $|\theta_{CW}|$, due to magnetic correlations. The feature at $T_N = 40 \text{ K}$ indicates the onset of long-range magnetic order, also consistent with previous observations.^{9,10} We emphasize that the large ratio $|\theta_{CW}|/T_N = 6.3$ clearly indicates that this is a magnetically frustrated material.

Additional information on the behavior of the magnetic correlations in the paramagnetic phase may be gained by

the temperature-derivative of the inverse susceptibility, $d(\chi(T) - \chi_0)^{-1}/dT$ [see Fig. 5(b)]. Again, a deviation of this curve from a constant (i.e., from the Curie-Weiss law) can be noticed below $\sim |\theta_{CW}|$. The inflection points of $(\chi(T) - \chi_0)^{-1}$ at $T \sim 160 \text{ K}$ and $T \sim 65 \text{ K}$, noticed in Figs. 5(a) and 5(b), are indicative of complex magnetic behavior in the paramagnetic phase, likely due to competing exchange interactions of different signs and/or magnitudes in this system. It is interesting to note that the fairly abrupt inflection point of $(\chi(T) - \chi_0)^{-1}$ at $\sim 65 \text{ K}$ coincides with the temperature below which anomalous phonon shifts were observed by Raman scattering.

IV. DISCUSSION

As described above, the phonon anomalies are clearly observable below $T^* \sim 60\text{--}65 \text{ K}$ for all samples, i.e., at T where no lattice anomaly or electronic phase transition has been reported. This severely limits the possible explanations for this phenomenon. Also, the feature on the magnetic susceptibility in BiMn_2O_5 at T^* [see Fig. 5(b)] suggests that the phonon shifts may be related to magnetism. In fact, to our present knowledge, the only feasible explanation for the observed anomalies at T^* appears to be rooted on the spin-phonon coupling. It is well known that the magnetic order and/or correlations may couple to the phonon frequencies through a modulation of the exchange integral by the lattice vibrations.^{26–29} The phonon frequency shift caused by this coupling is proportional to the spin pair correlation function $\phi = \langle S_i \cdot S_j \rangle$ and to the second derivative of the exchange integral with respect to the normal coordinate of the phonon.^{26,27,29} The first term depends directly on the T -dependent magnetic structure/correlations, while the second term may vary strongly with structural parameters such as the Mn-O-Mn superexchange angle and it is generally assumed to be T -independent. If anharmonic and/or structural contributions may be ignored or subtracted, the T -dependency of a relevant phonon frequency is a direct estimate of ϕ .

In conventional magnetic systems, ϕ and by extension the phonon shifts are negligible in the paramagnetic phase, except at T not exceeding T_N by more than few percents. However, in magnetically frustrated systems, a highly correlated paramagnetic state is typically formed above T_N .¹⁹ For RMn_2O_5 , the high-frequency phonons were assigned to Mn-O stretching vibrations, which are indeed prone to modulate the Mn-O-Mn superexchange interactions in this system,²⁷ supporting the spin-phonon mechanism. Thus, our results point to a scenario of remarkably strong magnetic correlations at T significantly above T_N , in agreement with the hypothesis of inherent magnetic frustration caused by the lattice geometry in this family.^{12,13} This hypothesis is further reinforced by the large frustration ratio ($|\theta_{CW}|/T_N = 6.3$) obtained for BiMn_2O_5 from magnetic susceptibility data (see above and Ref. 10). We note that a phonon softening on cooling due to the spin-phonon coupling in the paramagnetic state have been also recently reported on the frustrated system ZnCr_2O_4 .²⁹ Nonetheless, the rather complex crystal structure of RMn_2O_5 and unknown phonon eigenmodes pre-

vent a more quantitative analysis in the present case.

It is relevant to note that magnetic correlations have been observed in BiMn_2O_5 even at temperatures much higher than T^* (see Fig. 5). In fact, the magnetic correlations above T^* might also contribute to the phonon shifts through the spin-phonon mechanism. However, a presumably smooth T -dependence of such correlations would make the corresponding phonon shifts impossible to be separated from the shifts due to anharmonicity and thermal expansion. Thus, the new characteristic temperature T^* suggested by this work does not seem to mark the very onset of the magnetic correlations, however signaling a transition between states with correlations of distinct natures and/or strengths. The fairly abrupt inflection point of $(\chi(T) - \chi_0)^{-1}$ at $T \sim T^*$ may be another manifestation of such a transition.

An interesting feature of our results is the dependence with the R -ion of the phonon anomalies in the paramagnetic phase. While softenings are clearly observed for $R=\text{Bi}$ upon cooling below T^* , this tendency is much less pronounced for $R=\text{Eu}$, and is reversed to an anomalous hardening for $R=\text{Dy}$. This trend appears to be correlated with the ionic radii of the R ions, $r=1.17, 1.066, \text{ and } 1.027 \text{ \AA}$, for $R=\text{Bi}^{3+}, \text{Eu}^{3+}, \text{ and } \text{Dy}^{3+}$, respectively, under an eightfold coordination.³⁰ According to the spin-phonon interpretation, the different signs of the Raman shifts below T^* for $R=\text{Bi}$ and $R=\text{Dy}$, should be due to the change in sign of the $\langle S_i \cdot S_j \rangle$, at least for some Mn pairs. Thus, the paramagnetic correlations may be sensitive to the particular R -ion. We should mention that the low- T magnetic structures are also R -dependent, the magnetic propagation vectors for the studied samples being $(\sim 1/2, 0, k_z)$ with $k_z=1/2, 1/3, \text{ and } 1/4$ for $R=\text{Bi}, \text{Eu}, \text{ and } \text{Dy}$, respectively.^{9,13-15,31} It is not implausible to argue that the distinct magnetic correlations in the paramagnetic phase evidenced here is a precursor effect that leads to the distinct long-range-ordered magnetic structures below T_N . More detailed studies are certainly necessary to confirm or dismiss our suggestion.

Besides the unconventional behavior in the paramagnetic phase, phonon anomalies and/or changes of behavior have been also observed below T_c and/or T_N , however with opposite signs with respect to those between T_c/T_N and T^* . Indeed, for $R=\text{Bi}$ and Eu , softenings (hardenings) of the Mn-O stretching modes were observed below T^* (T_N), while, for $R=\text{Dy}$, the anomalous hardening of the mode at 705 cm^{-1} below T^* is transformed into a nearly constant behavior below T_c . In opposition to the anomalous phonon behavior in the paramagnetic phase discussed above, the origin of the phonon anomalies below T_c or T_N is ambiguous, and may be

twofold. The first possibility is again the spin-phonon coupling. In fact, the long-range magnetic order in this family may frustrate part of the exchange interactions,^{12,13} leading to a change of sign of $\langle S_i \cdot S_j \rangle$, at least for some i, j pairs. However, a discontinuous change of the phonon frequencies would be expected at T_N , rather than a change of behavior only. The second, and most likely, possibility are the phonon anomalies being a consequence of the Mn ionic displacements and/or lattice parameter anomalies that occur at the ferroelectric transition temperature, T_c .^{12,14} Concerning the second hypothesis, we should mention that the probable ferroelectric state for BiMn_2O_5 at low- T is not unambiguously established in the literature yet, although an anomaly in the dielectric constant was found at $T \sim T_N$.¹⁰

V. CONCLUSIONS

In summary, the high-frequency Mn-O stretching phonons in RMn_2O_5 ($R=\text{Bi}, \text{Eu}, \text{Dy}$) were investigated by means of Raman scattering, complemented by magnetic susceptibility measurements for $R=\text{Bi}$, with a focus on the paramagnetic regime. Our results reveal the existence of a new characteristic temperature for this family, $T^* \sim 1.5 T_N$, below which anomalous phonon shifts take place, likely related with magnetic correlations through the spin-phonon coupling mechanism. The sign and magnitude of the phonon shifts in the paramagnetic phase are different for each R -ion, indicating an evolution of the paramagnetic correlations with R . Such observations, together with the large frustration ratio ($|\theta_{CW}|/T_N=6.3$) obtained for BiMn_2O_5 , support magnetic frustration in this system, presumably caused by its complex lattice geometry. The phonon anomalies described here do not support a conventional behavior with a gradual enhancement of spin correlations upon cooling down to T_N , but rather suggests the establishment of a more interesting correlated magnetic state below T^* . The formation of a protorade of spin directors, such as found for the magnetically frustrated system ZnCr_2O_4 ,³² for example, cannot be discarded. In any case, the rich behavior of the magnetic correlations in the paramagnetic phase for this multiferroic family is certainly interesting, and deserves further investigation.

ACKNOWLEDGMENTS

The authors thank O. Agüero for helpful discussions. This work was supported by Fapesp and CNPq, Brazil, NSF DMR-0102235, U.S.A., Russian Foundation for Basic Research, Presidium of RAS, and Division of Physics of RAS.

*Electronic address: egranado@ifi.unicamp.br

¹N. A. Hill, J. Phys. Chem. B **104**, 6694 (2000).

²P. Curie, J. Phys. (Paris), Colloq. **3** (Ser. III), 393 (1894).

³I. E. Dzyaloshinskii, Sov. Phys. JETP **10**, 628 (1960).

⁴D. N. Astrov, Sov. Phys. JETP **11**, 708 (1960).

⁵N. Hur, S. Park, P. A. Sharma, J. S. Ahn, S. Guha, and S-W.

Cheong, Nature (London) **429**, 392 (2004).

⁶J. A. Alonso, M. T. Casais, M. J. Martínez-Lope, J. L. Martínez, and M. T. Fernández-Díaz, J. Phys.: Condens. Matter **9**, 8515 (1997).

⁷I. Kagomiya, K. Kohn, and T. Uchiyama, Ferroelectrics **280**, 297 (2002).

- ⁸N. Hur, S. Park, P. A. Sharma, S. Guha, and S-W. Cheong, *Phys. Rev. Lett.* **93**, 107207 (2004).
- ⁹A. Muñoz, J. A. Alonso, M. T. Casais, M. J. Martínez-Lope, J. L. Martínez, and M. T. Fernández-Díaz, *Phys. Rev. B* **65**, 144423 (2002).
- ¹⁰E. I. Golovenchits, V. A. Sanina, and A. V. Babinskii, *JETP* **85**, 156 July (1997).
- ¹¹S. Kobayashi, T. Osawa, H. Kimura, Y. Noda, I. Kagomiya, and K. Kohn, *J. Phys. Soc. Jpn.* **73**, 1593 (2004).
- ¹²L. C. Chapon, G. R. Blake, M. J. Gutmann, S. Park, N. Hur, P. G. Radaelli, and S-W. Cheong, *Phys. Rev. Lett.* **93**, 177402 (2004).
- ¹³G. R. Blake, L. C. Chapon, P. G. Radaelli, S. Park, N. Hur, S-W. Cheong, and J. Rodríguez-Carvajal, *Phys. Rev. B* **71**, 214402 (2005).
- ¹⁴V. Polyakov, V. Plakhty, M. Bonnet, P. Burlet, L.-P. Regnault, S. Gavrilo, I. Zobkalo, and O. Smirnov, *Physica B* **297**, 208 (2001).
- ¹⁵I. A. Zobkalo, V. A. Polyakov, O. P. Smirnov, S. V. Gavrilo, V. P. Plakatii, I. V. Golosovskii, and S. N. Sharygin, *Phys. Solid State* **38**, 725 (1996).
- ¹⁶D. Higashiyama, S. Miyasaka, N. Kida, T. Arima, and Y. Tokura, *Phys. Rev. B* **70**, 174405 (2004).
- ¹⁷K. Saito and K. Kohn, *J. Phys.: Condens. Matter* **7**, 2855 (1995).
- ¹⁸E. F. Bertaut, G. Buisson, S. Quezel-Ambrunaz, and G. Quezel, *Solid State Commun.* **5**, 25 (1967).
- ¹⁹A. P. Ramirez, *Handbook of Magnetic Materials* (Elsevier, New York, 2001), Vol. 13, pp. 423–520.
- ²⁰V. A. Sanina, L. M. Sapozhnikova, E. I. Golovenchits, and N. V. Morozov, *Sov. Phys. Solid State* **30**, 1736 (1988); E. I. Golovenchits, N. V. Morozov, V. A. Sanina, and L. M. Sapozhnikova, *ibid.* **34**, 56 (1992).
- ²¹The BiMn₂O₅ crystal was orientated arbitrarily with respect to the field. Note that, in Ref. 10 the magnetic susceptibility of BiMn₂O₅ was found to be isotropic in the paramagnetic phase.
- ²²D. L. Rousseau, R. P. Bauman, and S. P. S. Porto, *J. Raman Spectrosc.* **10**, 253 (1981).
- ²³B. Mihailova, M. M. Gospodinov, B. Güttler, F. Yen, A. P. Litvinchuk, and M. N. Iliev, *Phys. Rev. B* **71**, 172301 (2005).
- ²⁴The theoretical diamagnetic contribution was estimated with the usual relation $\chi_0^{jeo} = -0.79 \sum_i Z_i \langle r_i^2 \rangle / a_0^2 \times 10^{-6}$ (emu/mol), where Z_i is the total number of electrons of the i th ion in the formula unit, $a_0 = 0.529 \text{ \AA}$, and $\langle r_i^2 \rangle$ is the mean square electronic radius.²⁵ In this work, $\langle r_i^2 \rangle$ was estimated assuming a simple ionic model with uniform electron density inside a sphere defined by the Shannon crystal radius r_{i0} (Ref. 30). Thus $\langle r_i^2 \rangle = (3/5)r_{i0}^2$.
- ²⁵N. W. Ashcroft and N. D. Mermin, in *Solid State Physics* (Thomson Learning, 1976).
- ²⁶W. Baltensperger and J. S. Helman, *Helv. Phys. Acta* **41**, 668 (1968).
- ²⁷E. Granado, A. García, J. A. Sanjurjo, C. Rettori, I. Torriani, F. Prado, R. Sánchez, A. Caneiro, and S. B. Oseroff, *Phys. Rev. B* **60**, 11879 (1999); E. Granado, P. G. Pagliuso, J. A. Sanjurjo, C. Rettori, M. A. Subramanian, S-W. Cheong, and S. B. Oseroff, *ibid.* **60**, 6513 (1999); E. Granado, N. O. Moreno, H. Martinho, A. García, J. A. Sanjurjo, I. Torriani, C. Rettori, J. J. Neumeier, and S. B. Oseroff, *Phys. Rev. Lett.* **86**, 5385 (2001).
- ²⁸A. P. Litvinchuk, M. N. Iliev, V. N. Popov, and M. M. Gospodinov, *J. Phys.: Condens. Matter* **16**, 809 (2004).
- ²⁹A. B. Sushkov, O. Tchernyshyov, W. Ratcliff II, S. W. Cheong, and H. D. Drew, *Phys. Rev. Lett.* **94**, 137202 (2005).
- ³⁰R. D. Shannon, *Acta Crystallogr., Sect. A: Cryst. Phys., Diffr., Theor. Gen. Crystallogr.* **32**, 751 (1976).
- ³¹C. Wilkinson, F. Sinclair, P. P. Gardner, J. B. Forsyth, and B. M. R. Wanklyn, *J. Phys. C* **14**, 1671 (1981).
- ³²S-H. Lee, C. Broholm, W. Ratcliff, G. Gasparovic, Q. Huang, T. H. Kim, and S-W. Cheong, *Nature (London)* **418**, 856 (2002).